Phase-Shift Algorithm for Two Nonorthogonal Interferograms

2024 IEEE 3rd International Conference on Problems of Informatics, Electronics and Radio Engineering (PIERE) | 979-8-3315-1632-1/24/$31.00 ©2024 IEEE | DOI: 10.1109/PIERE62470.2024.10805078

Vladimir I. Guzhov
Faculty of Automation and Computer Engineering
Novosibirsk State Technical University
Novosibirsk, Russian Federation
vigguzhov@gmail.com

Sergey P. Ilinykh
Faculty of Automation and Computer Engineering
Novosibirsk State Technical University
Novosibirsk, Russian Federation
isp51@yandex.ru

Dmitry S. Khaidukov
Faculty of Automation and Computer Engineering
Novosibirsk State Technical University
Novosibirsk, Russian Federation
dmitriyhaydukov@gmail.com

***Abstract*—The phase step method is widely used to analyze interferograms and extract the phase distribution from them. Its limitation is the large number of interferograms required for this purpose. The minimum number is three interferograms. This paper describes a general analysis algorithm that requires only two interferograms, the phase shifts between which may not be orthogonal. The idea of the paper is to obtain an additional interferogram by transforming a two-dimensional elliptical cross section that is formed by the two interferograms into a three-dimensional cross section with respect to the base of some spatial cylinder. After determining the parameters of the ellipse, a projection vector parallel to the center axis of the cylinder is found. Then the two-dimensional section is projected onto a three-dimensional plane perpendicular to the center axis of the cylinder. Each of the projections of this plane onto the coordinate planes forms one of the interferograms. After obtaining three interferograms, phase demodulation was performed using a three-point algorithm. The RMS error of the phase calculation was 0.015 radians.**

Keywords—phase step, interferometry, elliptical trajectory, demodulation phase, measurement

I. Introduction

Optical interferometry is a fundamental technology in scientific research and engineering problems related to measuring not only the surface profile of transparent [1] or diffuse objects [2], but also their other parameters associated with changes in the phase distribution of the resulting interference patterns, such as index distribution of refractive index [3], displacement [4] and deformation [5], metrological measurements [6] diagnostics and data visualization in biomedicine [7] and many others. Phase Shift Interferometry (PSI) has been widely used because of its high sensitivity and repeatability of measurements. However, its limitation is the large number of interferograms required. The minimum number is three interferograms. In the paper we propose an approach allowing to use the PSI method with only two interferograms. This allows to reduce the time of registration of interferograms and, consequently, the time of measurements.

II. Theory

Optical interferometry is based on the comparison of two or more wave fronts in the visible light range (380-780 nm). One of the wave fronts is reflected by or passes through the test object, this wavefront is called the object wavefront, and the other wavefront reflected from the reference arm of the interferometer is called the reference wavefront. A change in the optical path difference (OPD) between the objective and reference wavefronts results in an interference pattern [8]. The intensity of the interference pattern (interferogram) can be represented

$$I(x,y) = a(x,y) + b(x,y)\cos(\phi(x,y)) + \varepsilon\,. \tag{1}$$

here $a(x,y)$ - background intencity, $b(x,y)$ - amplitude, $\phi(x,y)$ - phase of the recorded interference pattern.

Then the intensities of two non-orthogonal interferograms form an elliptic curve on the plane (x,y)

$$f(x,y) = \frac{(x_i - x_0)^2}{b_1^2} + \frac{(y_i - y_0)^2}{b_2^2} -$$

$$-2\frac{(x_i - x_0)(y_i - y_0)}{b_1 b_2}\cos\left(\phi_2 - \phi_1\right) = \sin^2\left(\phi_2 - \phi_1\right) \tag{2}$$

or

$$a_{11}x^2 + 2a_{12}xy + a_{22}y^2 + 2a_{13}x + 2a_{23}y + a_{33} = 0\,. \tag{3}$$

Let us represent this trajectory as a two-dimensional (flat) oblique section of some circular cylinder in three-dimensional space.

The idea of obtaining an additional interferogram is to transform this cross section into a three-dimensional cross section parallel to the base of the spatial cylinder. In this case, the base of the cylinder may not be parallel to the coordinate plane (see Fig. 1).

For this purpose, each point of the trajectory from the inclined plane is projected along the guide of the circular cylinder $\vec{L} = M - P$ onto the plane α, which is parallel to its base (Fig. 2). The elliptical trajectory is transformed into a circular trajectory, the phase shifts for which are known and are: $\delta_1 = -2\pi/3$, $\delta_2 = 0$ and $\delta_3 = 2\pi/3$ respectively. These values of phase shifts provide the maximum distance between phase shift angles in the range from 0 to 2π. This provides maximum robustness of the decoding algorithm to interference signal noise compared to other possible sets of phase shifts.

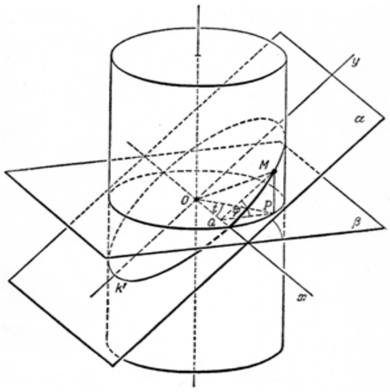

Fig. 1. Projection of the plane corresponding to the elliptical section onto the cylinder base plane.

The required transformation is performed as follows. At the first step, we determine the parameters of the ellipse and use them to find the guide of the cylinder, on the base of which the ellipse will be projected.

Let a – be the major semi-major axis of the ellipse, b – the minor semi-major axis of the ellipse. The semi-axis lengths of the ellipse can be determined from the equation of the principal invariant of the second-order curve [9] as follows: first, the roots of the characteristic equation λ are calculated from Eq.

$$\begin{vmatrix} a_{11}-\lambda & a_{12} \\ a_{12} & a_{22}-\lambda \end{vmatrix} = 0 . \tag{4}$$

The roots of this equation are the eigenvalues λ1 and λ2 of the real symmetric matrix

$$D = \begin{bmatrix} a_{11} & a_{12} \\ a_{12} & a_{22} \end{bmatrix} . \tag{5}$$

Then the lengths of the major and minor semi-axes of the ellipse at λ1> λ2 can be defined as:

$$a = \sqrt{(-1/\lambda_2)\cdot(A/D)} , \tag{6}$$

$$b = \sqrt{(-1/\lambda_1)\cdot(A/D)} , \tag{7}$$

where A and D are the second-order invariants of the curve calculated by the formulas [9]:

$$A = \begin{vmatrix} a_{11} & a_{12} & a_{13} \\ a_{12} & a_{22} & a_{23} \\ a_{13} & a_{23} & a_{33} \end{vmatrix} . \tag{8}$$

The guide vector of the cylinder $\vec{L}$ in which the ellipse is inscribed can be represented as follows:

$$\vec{L} = \begin{bmatrix} \cos(\Omega) \\ \sin(\Omega) \\ b/a \end{bmatrix} . \tag{9}$$

where Ω is the angle between the positive direction of the X-axis and the principal axis of the second-order curve, calculated by the formula [9]

$$\Omega = \frac{1}{2}\operatorname{arctg}\frac{2a_{12}}{a_{11}-a_{22}} . \tag{10}$$

Each point of the intensity trajectory is projected along the cylinder guide onto a plane that is parallel to the base of the cylinder. The transformation is performed as follows. Let $\vec{P}$ - be the radius-vector of the ellipse point on the original trajectory. Then the radius-vector of the point $\vec{G}$ corresponding to it on the circular trajectory is calculated as:

$$\vec{G} = \vec{P} - (\vec{L}\times\vec{P})\times\vec{L} . \tag{11}$$

The next step of the algorithm is to rotate the circular trajectory so that the direction of the normal of the plane in which the circular trajectory is located coincides with the direction of the unit vector $\vec{E}$. To perform this operation, it is necessary to find the matrix U of rotation of the normal of the plane to vector 3. Such a matrix can be found as follows. Let $\vec{T}$ be a vector that coincides with vector $\vec{P}$ in rotation. First, the angle β between vectors $\vec{T}$ and $\vec{P}$ is calculated by the formula

$$\beta = \arccos\frac{\vec{T}\cdot\vec{P}}{\left|\vec{T}\right|\cdot\left|\vec{P}\right|} . \tag{12}$$

We then calculate the vector product of these vectors:

$$\vec{R} = \vec{T}\times\vec{P} . \tag{13}$$

Normalize the vector $\vec{R}$

$$\vec{R} = \frac{\vec{R}}{\left|\vec{R}\right|} \tag{14}$$

and form the cosymmetric matrix Q :

$$Q = \begin{bmatrix} 0 & -R_z & R_y \\ R_z & 0 & -R_x \\ -R_y & R_x & 0 \end{bmatrix} . \tag{15}$$

Then the rotation matrix is found by Rodrigue's formula [10]

$$U = E + \sin(\beta)\cdot Q + (1-\cos(\beta))\cdot Q^2 , \tag{16}$$

where E is a unit matrix of dimension 3 × 3.
As a result of these operations, we obtain a set of three interferograms with known phase shifts $\delta_1 = -2\pi/3$, $\delta_2 = 0$ and $\delta_3 = 2\pi/3$, accordingly.

III. Simulation Rezults

The proposed algorithm was investigated by computer modeling method. The topogram of the test reflecting surface with the size of 512x512 samples was calculated by the formula

$$Z(x, y) = \sum_{i=0}^{4} \sum_{j=0}^{4} a_k x^i y^j \qquad (17)$$

where a_k - coefficients of the polynomial, $k \in [0,15]$.

On the Fig.2 shows the topogram of the reflecting surface calculated by formula (17).

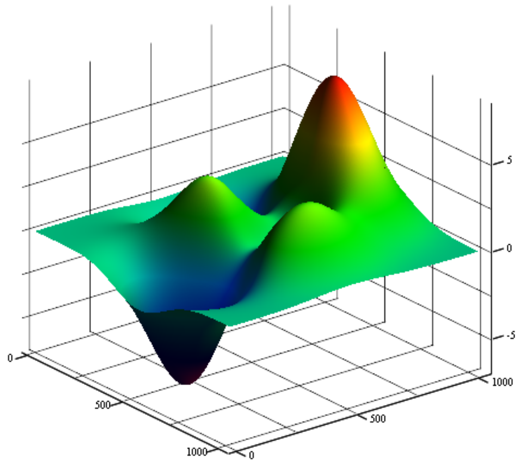

Fig. 2. Topogram of the test reflecting surface.

Phase ϕ of interference fringes calculated by the formula

$$\phi = \mathrm{mod}_{2\pi}\left(\frac{4\pi}{\lambda} Z\right). \qquad (18)$$

Fig. 3 shows the synthesized interference patterns with different phase shifts. The interference patterns contain saddle and elliptic features found in real interference patterns. Next, vectors composed from the interference patterns I_1 and I_2 (see Fig. 3) were formed.

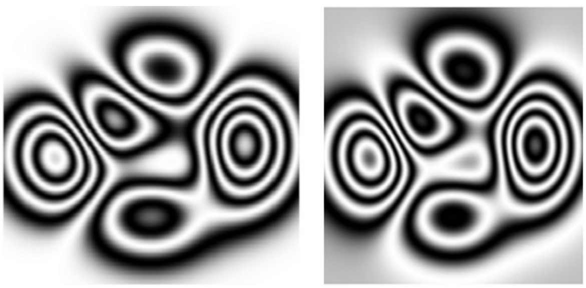

Fig. 3. Interference patterns forming an elliptical trajectory (from left to right) I_1 with phase shifts $\delta_1 = 0$ and I_1 $\delta_2 = \frac{\pi}{4}$, accordingly.

Then, using formulas (1) - (10), the ellipse parameters were calculated: the ratio of diameters of the principal axes and the direction of the principal axis. From them, the projection vector was determined by expression (8). Projection of vectors onto the base plane was performed by formula (11).

As a result, the transformed interference patterns were obtained, for which the phase shifts amounted to $\delta_1 = -2\pi/3$, $\delta_2 = 0$ and $\delta_3 = 2\pi/3$, top to bottom, accordingly (Fig. 4).

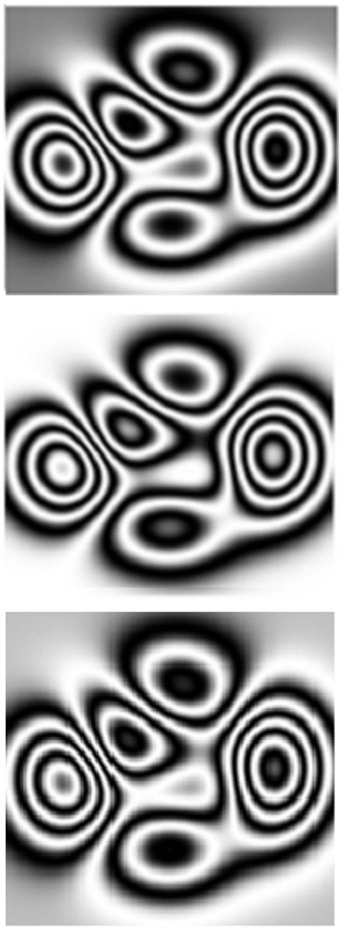

Fig. 4. Interference patterns with phase shifts , corresponding to the circular trajectory after interference pattern transformation (Fig. 3).

Demodulation phase of the obtained interference patterns was performed using the three-point formula [11]

$$\tan(\phi) = \frac{-\sqrt{3}\left(I_2 - I_3\right)}{I_2 + I_3 - 2I_1}. \qquad (19)$$

Note that by changing the position of the projection plane it is possible to obtain additional interferograms with other phase shifts. This allows us to use the decoding formulas with the number of points greater than three. The decoding error was estimated by calculating the root mean square error (RMSE)

$$\mathrm{RMSE} = \sqrt{\frac{\sum_{i=1}^{N} \left(\hat{y}_i - y_i\right)^2}{N}}, \qquad (20)$$

where $\hat{y}$ - calculated, and y - test values, accordingly.

The RMS error of the phase calculation was 0.015 radians, which, for example, at the study laser wavelength of 633 nm corresponds to the error of measuring the topogram heights of the measured object not more than 8 nm.

IV. CONCLASION

A method for finding an additional interferogram from two non-orthogonal interferograms is proposed. The method provides transformation of the elliptical trajectory formed by these interferograms to a circular form with known phase shifts. The transformation is performed by finding the plane on which the elliptic trajectory formed by the interference patterns with unknown phase shifts is projected as a circle. The algorithm is based on finding the circular section of a cylinder in which an elliptical trajectory is inscribed. The algorithm requires estimation of the principal direction and the ratio of principal and minor axes of the elliptic trajectory.

ACKNOWLEDGMENT

This work was financially supported by RNF grant 24-29-00006 “Development of Methods for Digital Holographic Interferometry”.

REFERENCES

[1] V. Shevchenko, A. Mialdun, V. Yasnou, Y. Lyulin, H. Ouerdane, V. Shevtsova, A. Mialdun, Y. Lyulin, V. Shevtsova, “Investigation of diffusive and optical properties of vapour-air mixtures: The benefits of interferometry,” Chemical Engineering Science, vol. 233(7). pp. 116433, 2021, [Online]. Available: http:10.1016/j.ces.2020.116433.

[2] A. Razzaghi, J. M. Amjad, M. Maleki, “Thickness measurement of transparent liquid films with Paraxial Self-Reference Interferometry,” Sci Rep, vol. 10, pp. 9240, 2020, [Online]. Available: http:10.1038/s41598-020-65799-z.

[3] A. Ushenko, A. Dubolazov, Zheng, O. Bakun, M. Gorsky, Yu. Ushenko, O. Litvinenko, I. Gordey, C. Zhebo, V. Sklyarchuk, “ Mueller matrix polarization interferometry of optically anisotropic architectonics of biological tissue object fields: the fundamental and applied aspects,” Frontiers in Physics, vol. 11, pp. 1-14, 2024.

[4] V. I. Guzhov, S. P. Ilinykh, I. A. Sazhin, E. N. Denezhkin, E. S. Kabak, D. S. Khaidukov, “Quasiheterodyne method of interference measurements,” Optoelectronics, Instrumentation and Data Processing, vol. 51 (3), pp. 280-286, 2015.

[5] V. I. Guzhov, S. P. Ilinykh, N. E. Kafidova, D. D. Bocharov, “Robust interferogram decoding algorithm,” Optoelectronics, Instrumentation and Data Processing, pp. 103–106, 2005.

[6] M. Servin, J. Quiroga, J. Padilla, “Fringe Pattern, Analysis for Optical Metrology: Theory, Algorithms, and Applications”. New York: Wiley, 2014.

[7] H. Majeed, S. Sridharan, M. Mir, L. Ma, E. Min, W. Jung, “Quantitative phase imaging for medical diagnosis,” J. Biophotonics, vol. 10, pp. 177–205, 2017.

[8] Optical Shop Testing. – 3rd ed.; [ed. Malacara D.]. New York: John Wiley and Sons, 2007.

[9] , G. A. Kornand, T. M. Korn Mathematical Handbook for Scientists and Engineers. McGraw-Hill Book Company, New York, USA, 1968.

[10] O. Rodrigues, “Des lois géométriques qui régissent les déplacements d’une système solide dans l’espace et de la variation des coordonnées provenant de ces déplacements considérés indépendamment des causes qui peuvent les produire,” Liouvillés Journ. Math, vol. 5, pp. 380–440, 1840.

[11] J. H. Bruning, D.R . Herriot, J. E. Gallagher, D. P. Rosenfeld, A. D. White, D. J. Brangaccio, “Digital wavefront measuring interferometer for testing optical surfaces and lenses,” Applied Optics,. vol. 13(11), pp. 2693-2703, 1974.